Use of ground penetrating radar for detecting underground holes in urban areas: XMU's experience

Zhiyou Hong*[1], Zhipeng Luo*[1] , Jonathan Li*[1,2], Zhenmiao Deng[1], Yiping Chen[1], Yu Zhang[1]

[1]Fujian Key Laboratory of Sensing and Computing for Smart Cites, School of Informatics, Xiamen University, Xiamen, Fujian 361005, China

[2]WatMos Lab, Faculty of Environment, University of Waterloo, Waterloo, Ontario N2L 3G1, Canada

junli@xmu.edu.cn; junli@uwaterloo.ca

ABSTRACT

Abstract - this paper presents a cosine-based back-projection(CBP) algorithm for ground penetrating radar(GPR) imaging to detect underground holes. Compared with the classic back-projection imaging algorithm, the CBP algorithm provides a better performance due to better effect of clutter suppression. In the proposed algorithm, a cosine-based measure function is established to describe the similar feature between every two different echo signals to achieve excellent artifact suppression. Then numerical simulation and experimental data set were used to test the SBP algorithm. The experimental data set was gained in Double Han Road, Siming District of Xiamen, China, and acquired by the the Latvia radar system, zond-12e model, which has a 115 kHz transmitting frequency, 40/80/160/320 Hz scanning frequency, ±40dB receive gain and 2000ns time-window width. The results fully demonstrate the effectiveness and superiority of CBP algorithm.

Keywords— ground-penetrating radar(GPR); radar imaging; cosine-based back-projection algorithm (CBP); measure function; artifact suppression

I. Introduction

As a promising non-destructive detection and imaging tool, ground penetrating radar (GPR) has advanced to a level where the subsurface condition of a roadway can be diagnosed with confidence[1], [2]. GPR uses short impulses of high frequency radio waves directed into the ground to acquire information about the subsurface. The energy radiated into the ground is reflected back to the antenna by features having different electrical properties to that of the surrounding material. To get more precise information about the hole, such as its depth, width and geometric, it is crucial to get data imaging by using echo signals. This paper therefore, presents a novel back-projection(BP) algorithm for GPR imaging to have better perspective on holes beneath Double Han Road.

The classical BP imaging algorithm[3]–[6] is one of the most practical imaging methods for its convenience and robustness, particularly when the imaging scene can be modeled as layered mediums. However, this algorithm offers limited capability for discriminating against artifacts. There are too much artifacts with high energy in the imaging result. And some of optimization imaging methods also have been advanced[7-9]. However, those imaging methods can only achieve the location of buried objects by brightness enhancing, and their imaging results is blurred between objects and background. They cannot obtain more information about objects parameters, and also have the shortcoming of the weak real-time performance. Torrione et al.[10] used histograms of oriented gradients to detect landmine in GPR data. And Windsor et al.[11] used generalized Hough transform to detect the location of buried objects. Hairu Zhang et al.[12] introduce the circular objects reconstruction algorithm to detect the location of buried objects. These methods just perform well in the object which has simple geometry.

In this paper, we propose a novel BP algorithm, which is with artifact suppression effect. A cosine-based method is introduced and a measure function is proposed to describe the similar feature between every two different echo signals in the classical BP algorithm. Simulation demonstrates the effectiveness of the proposed algorithm. And we also detect holes beneath Double Han Road by the method.

The remainder of this paper is organized as follows: Section 2 describes the CBP algorithm. Section 3 presents the experimental results and discussion. Section 4 concludes the paper.

II. THE CBP ALGORITHM

A. The classical BP algorithm

*——Corresponding author. Note: The first and second authors contributed equally to this work.

The 2-D imaging geometric model of the GPR system is shown in Fig 1. The scene is divided into two regions by z = 0. The upper region is air with permittivity $\varepsilon_1 = \varepsilon_0$, where ε_0 is the corresponding parameters in free space. The lower region is homogeneous earth with permittivity $\varepsilon_2 = \varepsilon_r \varepsilon_0$ where ε_0 is the relative permittivity of the soil. The directions of range and azimuth are the positive directions of Z axis and X axis, respectively. And the direction of scanning path is parallel to the X axis. The antennas transmit and receive signals in each of the M synthetic aperture positions. The currently concerned antenna position is represented by black rectangle with the sequence number k, whose coordinates are $(x_k, -h)$, while other $(M-1)$ antenna positions are represented by empty rectangles. There are three main steps to perform classical BP algorithm.

Firstly, for a arbitrarily given point A with coordinates (x_0, z_0) in the imaging area, the transmitting signal travels from $(x_k, -h)$ to (x_0, z_0), with a turning at the inflection point $(x_r, 0)$, and returns along the same path in reverse direction. The angles of incidence and refraction are denoted by θ_i and θ_t, respectively. Then according to Snell's law, we have:

$$\frac{\sin\theta_i}{\sin\theta_t} = \sqrt{\varepsilon_r} \tag{1}$$

One must to calculate the round-trip time delays from A to each of the M antenna positions. Time delays can be denoted as $\{t_{A,1}, t_{A,2}, \cdots, t_{A,M}\}$ and

$$t_{A,k} = \frac{2\sqrt{h^2 + (x_r - x_k)^2}}{c} + \frac{2\sqrt{z_0^2 + (x_0 - x_r)^2}}{c/\sqrt{\varepsilon_r}}, (k = 1, \cdots, M)$$

Secondly, the time delays are used to search out the response of point A in each of the M A-scans. The response is denoted as

$$S_i(t_{A,i}),\ (i = 1, \cdots, M) \tag{2}$$

Then we have an $M \times 1$ array for point A:

$$\{S_1(t_{A,1}), S_2(t_{A,2}), \cdots, S_M(t_{A,M})\} \tag{3}$$

Finally, the amplitude of point A in the final image will be formulated as

$$E_A = \sum_{i=1}^{M} S_i(t_{A,i}) \tag{4}$$

The above three steps will be repeated until all the points in the imaging scene are computed.

B. The CBP algorithm

The level of the artifacts' energy is quite high in the result of classic BP algorithm. In order to suppress the artifacts, We propose a novel BP algorithm based on cosine-based method. In our method, the $M \times 1$ response array for point A : $\{S_1(t_{A,1}), S_2(t_{A,2}), \cdots, S_M(t_{A,M})\}$ will not be summed directly as (4). We will first calculate

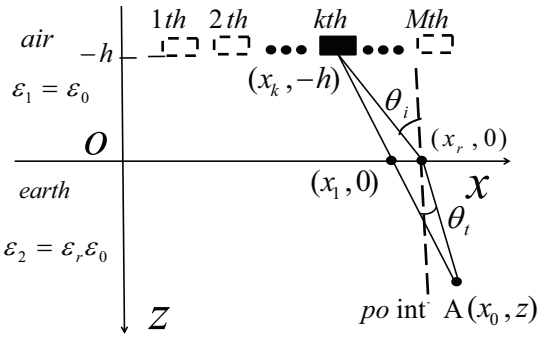

Fig. 1. Imaging geometric model

a measure function to describe the similar feature between every two different echo signals, then we will bring the function value as the weight to $S_i(t_{A,i})$, so a summation is made to get the imaging result of point A as follows

$$E_A = \sum_{i=1}^{M} \lambda_{A,i} S_i(t_{A,i}) \tag{6}$$

Where $\lambda_{A,i}$ is the weight of $S_i(t_{A,i})$.

B.1. measure function

For the S_i and S_j receiving signals, we denote a cosine function to describe the similar feature between them as fellow:

$$f(S_i, S_j) = \frac{\sum_{k=1}^{N}(\mathrm{S}_i(k) - \mathrm{M}_i)(\mathrm{S}_j(k) - \mathrm{M}_j)}{\sum_{k=1}^{N}(\mathrm{S}_i(k) - \mathrm{M}_i)^2)^{1/2} \sum_{k=1}^{N}(\mathrm{S}_j(k) - \mathrm{M}_j)^2)^{1/2})} \tag{9}$$

where $\mathrm{M}_l = \frac{1}{N}\sum_{k=1}^{N} S_l(k)$.

The measure function that is defined as above describes the similar feature between two signals. On one hand, we can observe that the more two signals have the similar feature, the larger the function value. On the other hand, if the two echo signals have the similar feature, it is clear to get that they contain more similar information, which is significant for us to get more precise information form them. So we take the weight of $S_i(t_{A,i})$ to $S_l(t_{A,l})$ as

$$\lambda_{l \leftarrow i} = f(S_l, S_i) \tag{10}$$

where $l \neq i$.

III. RESULTS AND DISCUSSION

The whole process was implemented in MATLAB. All experiments were performed on Windows 7 operating system.

A. Data pre-processing

GPR image is influenced by ground reflection, GPR diffraction and detector movement. Therefore, before further processing, it is necessary to carry out the pre-processing of noise and direct wave. We take the wavelet filter to finish the data pre-processing.

B. Numerical simulation

We use the GPRMAX2.0 to get the numerical experiment data.

The numerical experiment are carried out in a sandbox of 0.6 m ∗ 0.9 m (length ∗ width). The sandbox is filled with concrete. The relative dielectric constant of the concrete is 6.0. The electrical conductivity of the static medium of the concrete is 0.001 s/m. Its time_windows and the central frequency is 30×10^{-9} Hz and 900×10^{6} Hz, respectively.

In this numerical experiment, the round object is buried in concrete, as Fig. 2 shows. It is put along the z-axis. The depth of the center of the object is 0.275 m, and the diameter of the bottle's cross section is 0.001m. The height of antennas is 0cm.

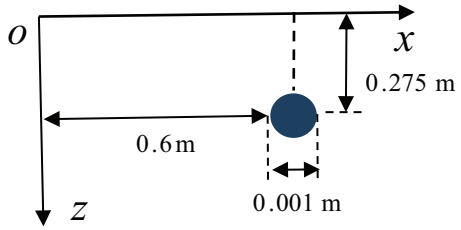

Fig. 2 Geometry of the imaging scene

Fig. 3 shows the imaging results of the classic BP algorithm and the CBP algorithm, respectively. The rue positions of objects can be marked by the two algorithm. However, it is obvious that Fig. 3(a) has much more artifacts than that in Fig. 3(b). In order to quantitatively describe the effect of artifact suppression, we evaluate the imaging quality by integrated sidelobe ratio (ISLR), which is defined as:

$$ISLR = 10 \log_{10}\left(\frac{E_{total} - E_{main}}{E_{main}}\right) \qquad (11)$$

where E_{total} and E_{main} are the energies of the whole image and the main lobe of the object. The calculated ISLRs for Fig. 3(a) and 3(b) are −4.9 dB and −42.8 dB, respectively; the ISLR decreases by 37.9 dB.

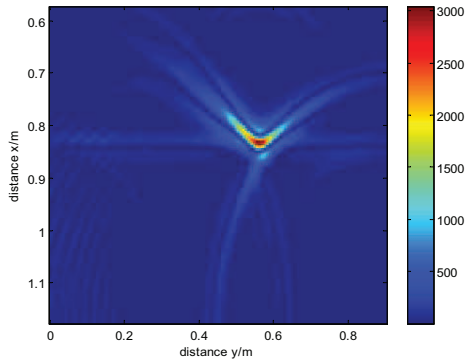

(a)

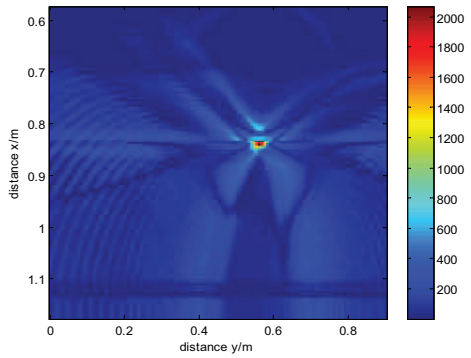

(b)

Fig.3. Comparison of imaging results for the numerical simulation. (a) Result of classic BP algorithm. (b)Result of the CBP algorithm.

C. Experimental data test

The experimental data set was gained in Double Han Road, Siming District, city of Xiamen, China, and acquired by the Latvia radar system, zond-12e model, which has a 115 kHz transmitting frequency, 40/80/160/320 Hz scanning frequency, ±40dB receive gain and 2000ns time-window width.

Fig. 4 shows the GPR imagery. Imaging results of the classic and the CBP algorithm are shown in Fig. 5. It is very likely that there is a hole under the selected sections of the Double Han Road. It is obvious that the CBP algorithm has better performance.

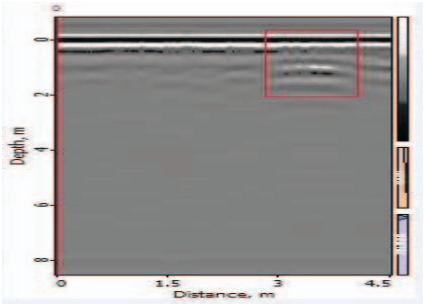

Fig. 4. one of the radar images experimental data

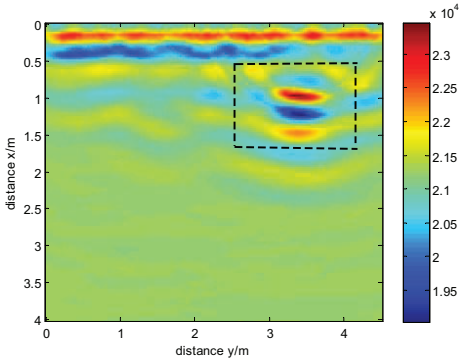

(a)

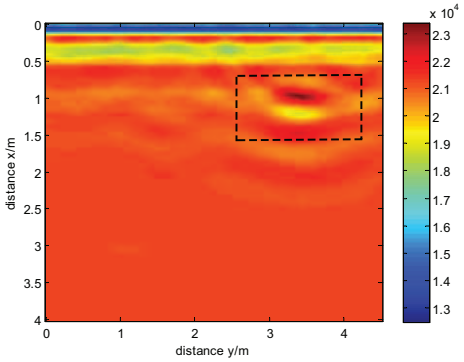

(b)

Fig5. Comparison of imaging results for the experimental data test. (a) Result of classic BP algorithm. (b) Result of the CBP algorithm.

IV. CONCLUSION

In this paper, we have presented CBP algorithm for radar imaging, and the proposed algorithm has dramatically suppressed the artifacts in the imaging result of the classic BP algorithm by using the cosine-based information of the receiving data. The application of the proposed algorithm is practically valuable in the imaging of underground objects with high quality. This study is meaningful for governments, decision makers and urban planners, who need the knowledge of urban roads to formulate correct and effective urban development policy.

REFERENCES

[1] M. Grasmueck, R. Weger, H. Horstmeyer, "Full-resolution 3D GPR imaging for geoscience and archeology". In 10th International Conference on Ground Penetrating Radar.pp. 329-332, 2004

[2] S. Yi, H. Chunlin, and L. Wentai. Theory and Applications of Ground Penetrating Radar. Beijing, China: Sci. Press, 2006.

[3] J. I., Halman, K. Shubert, G. T. Ruck, "SAR processing of ground-penetrating radar data for buried UXO detection: results from a surface-based system". IEEE Trans. Antennas -Propag, vol. 46, no., pp. 1023-1027,1998.

[4] L. Carin, N. Geng, M. Mcclure, "Ultra-Wideband Synthetic Aperture Radar for Mine Field Detection". IEEE Antennas -Propag. Mag., vol.41,no.,pp. 18-33, 1999.

[5] L. Chen, O. Shan. "A time-domain beamformer for UWB through-wall imaging". TENCON 2007, IEEE, pp. 1-4, 2007 .

[6] L Zhou, Y Su. "A GPR imaging algorithm with artifacts suppression". International Conference on Ground Penetrating Radar. pp. 1-7, 2010.

[7] Y. Jungang, J. Tian, H. Xiaotao. "Sparse MIMO array forward-looking GPR imaging based on compressed sensing in clutter environment". IEEE, pp. 4480-4494, 2014.

[8] M. Razavian, M. H. Hosseini, R. Safian. "Time-Reversal Imaging Using One Transmitting Antenna Based on Independent Component Analysis". IEEE pp. 1574-1578, 2014.

[9] Xuan Feng, Motoyuki Sato, CaiLiu. "Subsurface imaging using a handheld GPR MD system". IEEE pp. 659-662, 2012.

[10] P. A.Torrione, K. D.Morton, R.Sakaguchi. "Histograms of Oriented Gradients for Landmine Detection in Ground-Penetrating Radar Data". IEEE, pp. 1539-1550, 2014.

[11] C. G.Windsor, L.Capineri, P.Falorni. "A Data Pair-Labeled Generalized Hough Transform for Radar Location of Buried Objects". IEEE, pp. 124-127, 2014.

[12] H. Zhang, S. Ouyang, G. Wang. "A novel reconstruction algorithm for circular object in ground penetrating radar data". IEEE, pp. 3781-3789, 2015.